Journal of Applied Electrochemistry **32**: 1019–1027, 2002.

Electrodeposition of cobalt from gluconate electrolyte

S.S. ABD EL REHIM, MAGDY A.M. IBRAHIM* and M.M. DANKERIA
Chemistry Department, Faculty of Science, Ain Shams University, Cairo, Egypt
*(*author for correspondence)*

Received 5 November 2001; accepted in revised form 14 May 2002

Key words: chronoamperometry, cobalt deposition, current efficiency, microhardness, morphology, potentiodynamic, throwing power

Abstract

Cobalt electrodeposited onto steel substrate was carried out from solutions containing cobalt sulfate, boric acid and sodium gluconate. The study dealt with the influence of bath composition, current density, pH and temperature on the potentiodynamic cathodic polarization curves, cathodic current efficiency, and throwing power, as well as the throwing index of these baths. The microhardness of cobalt electrodeposited from gluconate baths is generally high and higher than that of cobalt deposited under similar conditions from sulfate, chloride, bromide and acetate baths. The surface morphology of the as-deposited cobalt was investigated using scanning electron microscopy (SEM) while the structure was studied using X-ray diffraction analysis. Cyclic voltammetric, as well as current-transient, techniques recorded on a glassy carbon electrode suggested that the deposition of cobalt from gluconate bath occurs via a nucleation process under charge transfer control.

1. Introduction

Electrodeposited cobalt and cobalt alloys are widely employed throughout the computer industry as the recording media in both magnetic drum and magnetic tape memory systems [1, 2]. In addition, the magnetic properties of electrodeposited cobalt based alloys, has attracted increasing attention [3–6]. Dennis et al. electrodeposited cobalt [7] and Co alloys coatings from cobalt Watts plating bath containing sodium heptonate as a complexing agent [8]. However, compared to the many technical applications in industry for cobalt electrodeposits, few studies have been made on cobalt electrodeposition.

Cobalt deposition has been carried out on different substrates such as nickel, vitreous carbon and copper, and from different baths containing chloride or sulfate aqueous solutions [2, 9–11], citrate solution [12], triethylene diamine, cobalt(III) chloride in 30% KOH, solutions of cobalt(II) thiocyanate in *N*,*N*-dimethyl formamide [13, 14], Co(II) in ammonium chloride aqueous solutions [15, 16]. More recently the crystallographic structure of electrodeposited Co film obtained from an aqueous bath with five organic solvents (ethanol, formamide, *N*-methyl formamide, *N*,*N*-dimethyl formamide and dimethyl sulfoxide) bath were studied [17].

The present research aims to develop new baths for producing good quality cobalt deposits, which have the advantage of being more environmentally friendly than traditional baths. In addition, the investigation aims to throw more light on the mechanism of cobalt electrodeposition from gluconate baths.

2. Experimental details

All the plating baths and reagents were made from Analar chemicals without further purification and doubly distilled water. For electrodeposition, a steel cathode and platinum sheet anode, both of dimensions 2.5 cm × 3.0 cm, were used. The platinum sheet was surrounded by an asbestos diaphragm to preclude oxidation of Co^{2+} ions and errors in the measured potentials caused by oxygen evolved at the anode. The plating cell used was a rectangular Perspex trough (10 cm × 3 cm) provided with vertical grooves, on each of the side walls, to fix the electrodes. Before each run, the steel cathode was mechanically polished with different grade emery papers (600, 800, 1000 and 1500) and then washed with distilled water, rinsed with ethanol and weighed. Direct current was supplied by a d.c. power supply unit (GPS-3030D). The cathodic current efficiencies (f) were determined with the help of a Cu-coulometer ($f = w_{exp}/w_{th}$) where w_{exp} is the weight of the deposit obtained experimentally and w_{th} is the weight of the deposit calculated theoretically according to Faraday's law. Electrodeposition was carried out for 15 min in each case.

The percentage throwing power (P_{throw}) of the solution was measured using a Haring–Blum rectangular Perspex cell (3.0 cm wide, 13.0 cm long, with 2.5 cm

solution depth) fitted with one anode between two parallel steel cathodes where the ratio of the far to the near distance was 5:1. This was calculated from Field's formula [18]:

$$P_{\text{throw}} = \frac{l - m}{l + m - 2} \times 100 \quad (1)$$

where l is the ratio of the cathode distance to the anode distance (far to near, $l = 5$) and m is the ratio of the weight of the deposited metal on the near to the weight of the metal deposited on the far cathode. The values of m were measured as a function of l over a wide range of linear ratios varying between 1:1 and 5:1. The throwing index (I_{throw}) of each bath was considered as the reciprocal of the slope of the m against l plot [19, 20].

Potentiodynamic cathodic polarization curves were recorded using steel substrates by sweeping the potential from the rest potential in the negative direction at a scan rate of 10 mV s^{-1}. On the other hand, the cyclic voltammetry measurements were recorded on a glassy carbon working electrode (area 0.1963 cm^2) starting from the open circuit potential to the more negative direction up to −1.2 V and then reversed at the same scan rate in the positive direction up to the anodic potential 0.5 V. The carbon electrode was polished before each run with diamond paste (0.25 μm) until a mirror surface was obtained, then washed several times with doubly distilled water. A potentiostat/galvanostat (EG&G model 273) controlled by a computer was used for all the electrochemical measurements. All potentials were measured relative to a saturated calomel electrode (SCE). To avoid contamination, the reference electrode was connected to the working cathode via a bridge provided with a Luggin–Haber tip and filled with the solution under test.

The surface morphology of the Co electrodeposited on steel was examined using scanning electron microscopy (Joel–JEM 1200 EX II electron microscope). The crystalline structure of the Co thin film deposited on steel from the optimum bath under different operating conditions was examined by X-ray diffraction using a Philips PW 1390 diffractometer (40 kV, 20 mA) with Ni filter and CuK_α radiation. The microhardness of these deposits (thickness > 10 μm) was measured by means of a microhardness tester. A 25 kg (250 N) load was applied for 30 s. 10 replicated hardness measurements were used for the estimation of microhardness values. The average hardness values were expressed as Vickers (H_v) in kg f mm^{-2} (note: 1 kg f $mm^{-2} \equiv 10$ MPa).

3. Results and discussion

Cobalt electrodeposition on steel was carried out from solutions containing cobalt sulfate, boric acid and sodium gluconate. The composition, conductivity and pH of the gluconate baths are given in Table 1. Cobalt sulfate is used as a source for Co^{2+} ions while sodium gluconate is used as a complexing agent. Boric acid is commonly added to nickel and cobalt plating baths as a buffer to control the pH at the cathode–solution interface [21].

3.1. *Potentiodynamic cathodic polarization curves*

In acidic solutions (pH < 7), and in the presence of sodium gluconate, Co^{2+} is present mainly as

Table 1. Composition and pH of the investigated electroplating baths

Bath	Concentration/g dm^{-3}			$C/\Omega\ cm^{-1}$	pH
	$CoSO_4 \cdot 7H_2O$	H_3BO_3	$NaC_6H_{11}O_7$		
Co1.a	20	30	50	14.1	3.95
Co1.b	40	30	50	18.0	3.70
Co1.c	60	30	50	21.3	3.60
Co1.d	80	30	50	24.1	3.55
Co1.e	100	30	50	26.9	3.50
Co1.f	120	30	50	29.6	3.45
Co1.g	140	30	50	32.2	3.35
Co2.a	100	30	0	23.3	3.95
Co2.b	100	30	10	24.4	3.50
Co2.c	100	30	20	25.1	3.40
Co2.d	100	30	30	26.2	3.45
Co2.e	100	30	40	26.3	3.48
Co2.f	100	30	50	26.7	3.50
Co2.g	100	30	60	26.8	3.60
Co2.h	100	30	100	25.8	3.55
Co3.a	100	0	50	27.2	5.35
Co3.b	100	10	50	27.0	3.60
Co3.c	100	20	50	26.9	3.50
*Co3.d	100	30	50	26.7	3.50
Co3.e	100	40	50	26.4	3.45
Co3.f	100	50	50	26.1	3.40

* Selected optimum bath composition.

$[Co(C_6H_{11}O_7)]^+$ complex. It has been suggested that the gluconate ion is attached to Co^{2+} by coordination through the carboxyl group and one of the adjacent hydroxyl groups [22]. Therefore, cobalt may be obtained by electroreduction of either the complexed or uncomplexed ions with simultaneous hydrogen evolution as a side reaction.

Figure 1 shows that the potentiodynamic cathodic polarization curve from solution containing only 50 g dm^{-3} sodium gluconate and 30 g dm^{-3} boric acid at pH 3.5 and at 25 °C (curve (a)) exhibits a low limiting current density which corresponds principally to hydrogen evolution. However, addition of Co^{2+} ions causes drastic changes to the cathodic polarization. In this case, there is a gradual increase in the current with increasing potential up to a certain potential at which the current rapidly increases. Therefore, the potential at which the current rises rapidly is considered as the deposition potential of cobalt. At potentials equal to, or higher than, this deposition potential, both deposition of cobalt and evolution of hydrogen occur simultaneously. Consequently, the predicted percentage cathodic current efficiency (*f*) for metal deposition is less than 100%. Reduction of the cobalt gluconate complex is not as easy as the reduction of free Co^{2+} ions. This is the reason for the high polarization observed during Co electrodeposition from the gluconate baths as shown in Figures 1–4. The data in Figure 1 also show that increase in Co^{2+} concentration shifts the deposition potential of cobalt to less negative values most probably as a result of an increase in the relative concentration of Co^{2+}, particularly in the cathode diffusion layer, and this is reflected in a decrease in the concentration polarization associated with cobalt deposition. The reverse was observed by increasing the concentration of sodium gluconate in the bath, as shown in Figure 2. In other words, the cathodic polarization increases with increase

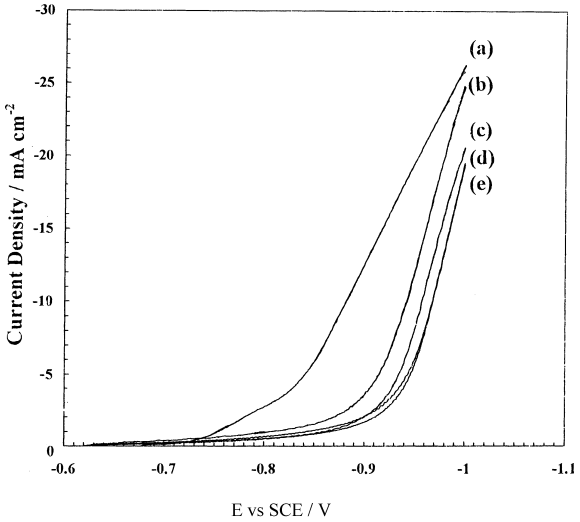

Fig. 2. Potentiodynamic cathodic polarization curves during Co electrodeposition; curves: (a) bath Co2.a, (b) bath Co2.c, (c) bath Co2.f, (d) bath Co2.g and (e) bath Co2.h.

in gluconate concentration as a result of increasing the stability of the cobalt gluconate complex formed.

The potentiodynamic cathodic polarization curves for cobalt deposition at different boric acid concentrations were studied and the results showed that, as the boric acid concentration increases, there is a reduction in the deposition potential of cobalt (data is not included here). Boric acid facilitates the deposition of cobalt.

Figure 3 displays the influence of pH (pH 2.0–5.0) on the cathodic polarization curves. The pH of each bath was adjusted by adding concentrated H_2SO_4 or NaOH solution. The potentiodynamic cathodic polarization curve is shifted significantly negatively with increasing pH. This trend may be related to an increase in hydrogen overpotential. Moreover, in acidic solutions, the Co^{2+} ions are bound into the complex via a ligand

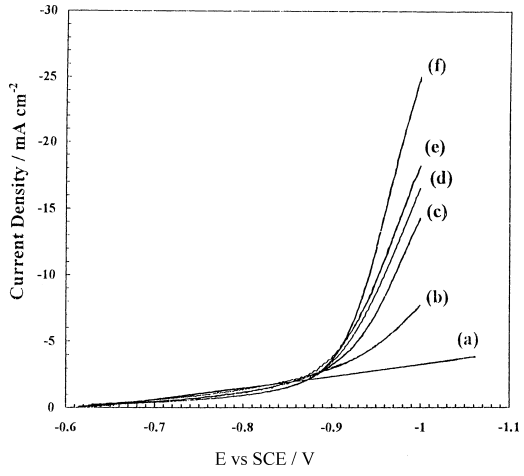

Fig. 1. Potentiodynamic cathodic polarization curves during Co electrodeposition; curves: (a) 50 g dm^{-3} sodium gluconate + 30 g dm^{-3} boric acid, (b) bath Co1.a, (c) bath Co1.b, (d) bath Co1.c, (e) bath Co1.d, and (f) bath Co1.e.

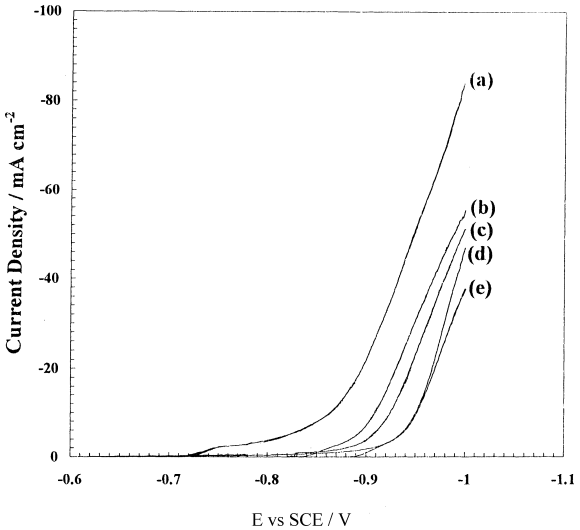

Fig. 3. Potentiodynamic cathodic polarization curves during Co electrodeposition from the optimum bath Co3.d at different pH; curves: (a) 2.0, (b) 3.0, (c) 3.5, (d) 4.0 and (e) 5.0.

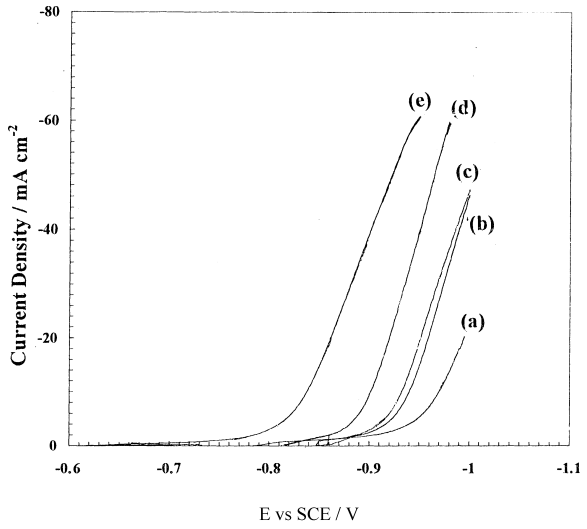

Fig. 4. Potentiodynamic cathodic polarization curves during Co electrodeposition from the optimum bath Co3.d at different temperatures; curves: (a) 10 °C, (b) 20 °C, (c) 25 °C, (d) 40 °C and (e) 50 °C.

carboxyl group, and of the adjacent hydroxyl group [23], but on increasing pH, coordination on the secondary alcoholic group is followed by liberation of a proton. Formation of a chelate ring is also possible [23]. These processes lead to an increase in cathodic polarization.

The effect of electrolyte temperature on the potentiodynamic cathodic polarization curves is shown in Figure 4. An increase in temperature decreases the cathodic polarization due to its influence on the activation overpotential for the reducible ions. Moreover, an increase in temperature may change the relative abundance of both complexed and uncomplexed Co^{2+} ion in the solution. It seems that a rise in temperature decreases the stability constant of the complex species and thus enhances the existence of relatively higher concentrations of the uncomplexed Co^{2+} ions.

3.2. *Cathodic current efficiency*

The percentage cathodic current efficiency f for cobalt plating from all gluconate baths (Co.1a–Co.3f, see Table 1) was determined. The efficiency determined from these baths is less than 100% (81–94%) as a result of simultaneous hydrogen evolution. However, f is similarly high to that of sulfate baths [11] but higher than that for citrate baths [12]. The efficiency f increases from 62% to 91% with increasing cobalt salt concentration from 20 to 60 g dm^{-3}. Further increase in the concentration of cobalt salt has no significant effect on f. Similarly, f increases from 89% to 94% with increasing sodium gluconate concentration from 10 to 50 g dm^{-3}. Moreover, f increases from 83% to 94% with increasing boric acid concentration from 10 to 50 g dm^{-3}. These data show that the presence of boric acid in the bath improves the efficiency of Co deposition. In this case, boric acid plays a greater role than merely as a buffer. It is now believed that boric acid complexes with Co^{2+} ions acting as a homogeneous catalyst or adsorbs on the electrode surface [24–26] which lowers the overpotential for cobalt deposition. Horkan [27] suggested that boric acid is adsorbed on the cathode surface, and thus decreases the active area for hydrogen evolution, thus affecting the resulting morphology characteristics of the deposits.

Smooth, compact and highly adherent cobalt deposits were obtained from Co.3d bath. Therefore, this bath was selected as the optimum bath for further investigation.

One of the most important operating conditions in an electroplating process is the current density. Increasing the current density to 2 A dm^{-2} greatly improves f, thereafter the efficiency tends to level off (Figure 5(a)). The whole current density range studied for cobalt deposition includes a component due to hydrogen evolution at cathode surface.

The effect of pH on percentage cathodic current efficiency f of cobalt electroplating from the optimum bath is given in Figure 5(b). The cathodic current efficiency increases sharply and then tends to level off with increasing pH. Clearly hydrogen evolution is dominant at low pH. These results are consistent with cathodic polarization data (Figure 3).

The effect of temperature on the percentage current efficiency f of cobalt deposited from the optimum bath is given in Figure 5(c). An increase in temperature from 20 °C to 70 °C decreases the cathodic current efficiency from 95% to 80%. Further increase in temperature has no remarkable influence on f but the deposits tend to be black.

It is found that the efficiency of cobalt plating increases slightly from 84% to 92% with increasing plating time from 5 to 15 min. With further increase in plating time there is no significant change. Increase in f with plating time may be attributed to the fact that hydrogen evolution takes place simultaneously with cobalt deposition. Hydrogen evolution decreases with increasing plating time as a result of increasing pH in the vicinity of the cathode surface.

From the above results, it is found that the optimum operating parameters for plating adherent and bright cobalt deposits from the optimum bath (Co.3d) are: pH 3.5, current density 2.0 A dm^{-2} and 25 °C.

3.3. *Cyclic voltammetry*

In these experiments, Co was deposited on a glassy carbon electrode instead of steel to avoid dissolution of steel during the anodic scan. Typical cyclic voltammograms recorded at glassy carbon using the optimum (Co3.d) bath are shown in Figure 6. The voltammograms were swept starting from the open circuit potential in the more negative direction up to −1.2 V and then reversed at the same scan rate up to an anodic potential of 0.5 V. In negative going scan, the cathodic current increases suddenly at −900 mV (deposition potential of Co) without any limitation indicating that the reduction

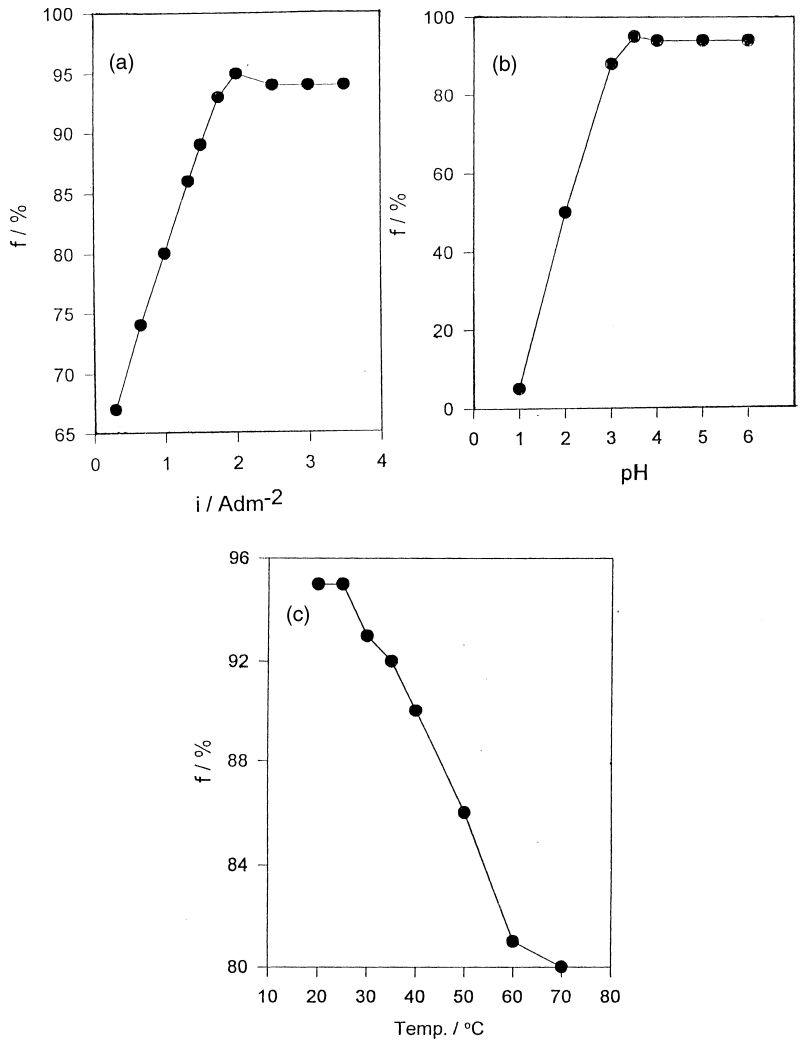

Fig. 5. Dependence of percentage cathodic current efficiency f on different operating conditions.

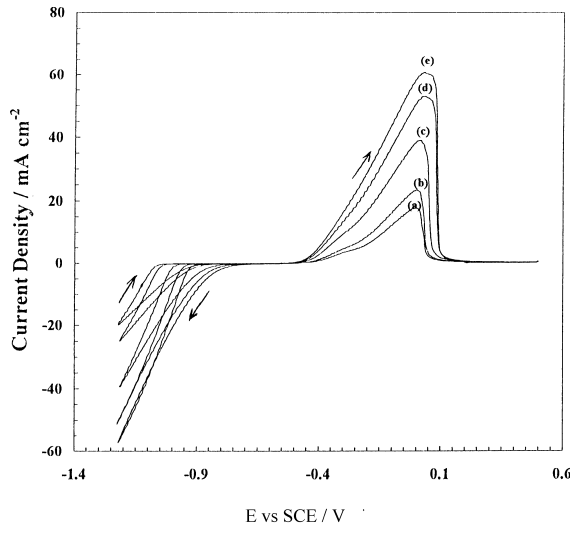

Fig. 6. Cyclic voltammetry recorded at glassy carbon electrode for Co3.d bath at different temperatures (scan rate 50 mV s^{-1}); curves: (a) 10 °C, (b) 20 °C, (c) 30 °C, (d) 40 °C and (e) 50 °C.

of Co is under charge transfer control. This confirms the suggestion that the deposition of cobalt from the gluconate bath occurs via a nucleation process under charge transfer control. On reversing the potential scan, the cathodic current gradually decreases as the reverse scan goes in the anodic direction and exhibits crossover between the cathodic and anodic current at a crossover potential E_c at about −0.57 V [28]. The deposition of cobalt from aqueous chloride solutions gives similar results [29]. Before the crossover potential, the return sweep cathodic current is always higher than the cathodic current on the forward scan. This trend is mainly related to the change in pH at the electrode surface. Progressive evolution of hydrogen ions leads to an increase in pH at the electrode surface. The increasing pH improves the current efficiency of cobalt deposition (see Figure 5(b)). Theoretically, the crossover potential, E_c, should correspond to the reversible potential E° of cobalt deposition −0.277 V [30]. The difference between the experimental value −0.57 V and the theoretical value may be assigned to hydrogen evolution.

However, the anodic excursion span exhibits one anodic peak. This peak is related to the anodic stripping of cobalt previously deposited on the glassy carbon. The

anodic stripping charge (the area under the peak) under the prevailing conditions can be taken as a qualitative measure of the amount of cobalt deposited [25]. Moreover, Figure 6 shows that the anodic stripping charge increases greatly with increasing electrolyte temperature, which indicates that the cathodic current efficiency for cobalt deposition from gluconate bath on glassy carbon increases with temperature. This trend is not consistent with the data shown in Figure 5, where the cathodic current efficiency decreases with temperature. This contradiction may be related to the variation in the cathodic material, since in Figure 5(c), the deposition occurs on steel.

3.4. *Current–time transient (chronoamperometric) measurements*

A series of current–time transient measurements for cobalt deposition at a given deposition potential E_s from gluconate baths on glassy carbon electrode was conducted. Figure 7 shows typical potentiostatic current–time transients for cobalt deposition from the optimum bath (Co.3d) at pH 3.5, 25 °C at various deposition potentials. It is seen that the current increases rapidly to a limiting or steady state current (i_s) at a time (t_s). Such transients are characteristic of the nucleation and phase growth of a metal on glassy carbon. Moreover, the data suggest that the nucleation growth is not a diffusion-controlled process. The rising portion of the curve reflects the rise in current as the electroactive area increases either as each independent nucleus grows in size (instantaneous growth) and/or the number of nuclei increases (progressive growth). The current transients level off when the exposed surface becomes completely saturated [31]. The small variation of the steady state current with time suggests that after overlapping of the growth nuclei and formation of a continuous layer, thickening takes place under partial diffusion control. The steady state current, i_s, increases and the time scale of the transient decrease as the deposition potential is made more negative. Hydrogen evolution again occurs but the current for this side reaction serves only to amplify the response without changing its shape [32].

The rising parts of the transients, were analysed [33] by plotting $i^{1/2}$ against t, whereby straight lines were obtained as shown in Figure 8. This indicates that the cobalt deposit is formed by a mechanism where instantaneous nucleation is followed by 3D growth under charge transfer control. This means that the formation of fresh nuclei is arrested at a very early stage. The slopes of these plots are proportional to the rate constant for charge transfer [33].

3.5. *Throwing power and throwing index of the bath*

The values of the percentage throwing power P_{throw} of the bath computed by Field's empirical formula at a distance ratio 1:5 were determined. Moreover, the throwing index I_{throw} were determined by plotting the metal distribution ratio m, and the linear ratio l (1:1–1:5) as shown in Figure 9 as a representative example. The reciprocal of the slopes of these lines are called the throwing index I_{throw} and represent a measure of bath throwing power [19]. P_{throw} decreases from 11.1% (Co1.a bath) to 6.8% (Co1.c bath) as the cobalt salt in the bath increases from 20 to 60 g dm^{-3}. The corresponding I_{throw} values are 1.25 and 1.14, respectively. The decrease in P_{throw} is due to the observed decrease in cathodic polarization with increasing Co^{2+} concentration (Figure 1). The data reveal also that P_{throw} decreases from 5.9% (Co2.f bath) to −8.4% (Co2.h bath) as the concentration of sodium gluconate increases from 50 to 100 g dm^{-3}. The corresponding I_{throw} values are 1.10 and 0.88, respectively. Also, the effect of boric acid

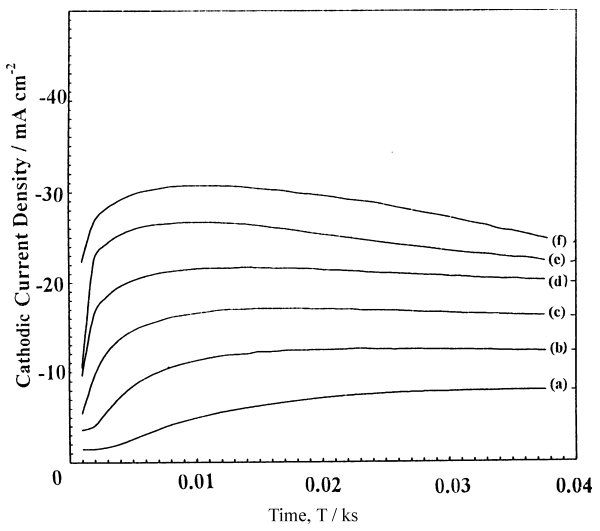

Fig. 7. Potentiostatic current–time transients from Co3.d bath at various cathodic deposition potentials, curves: (a) −1000, (b) −1050, (c) −1100, (d) −1150, (e) −1200 and (f) −1250 mV.

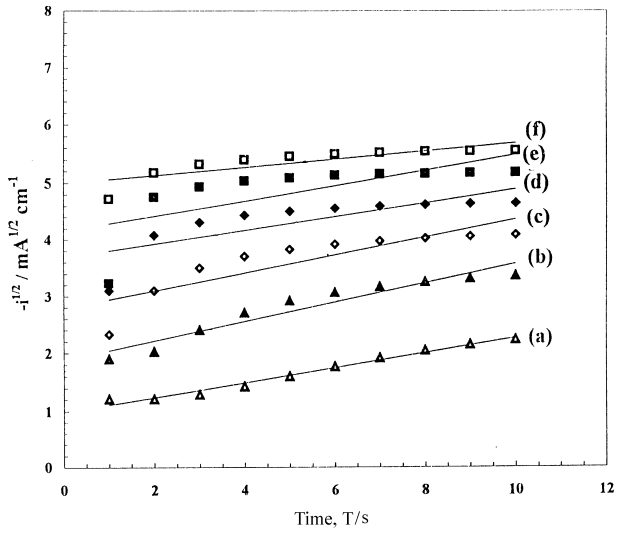

Fig. 8. Dependence of $i_{1/2}$ on the time t for cobalt deposited from Co3.d bath at various cathodic deposition potentials, curves: (a) −1000, (b) −1050, (c) −1100, (d) −1150, (e) −1200 and (f) −1250 mV.

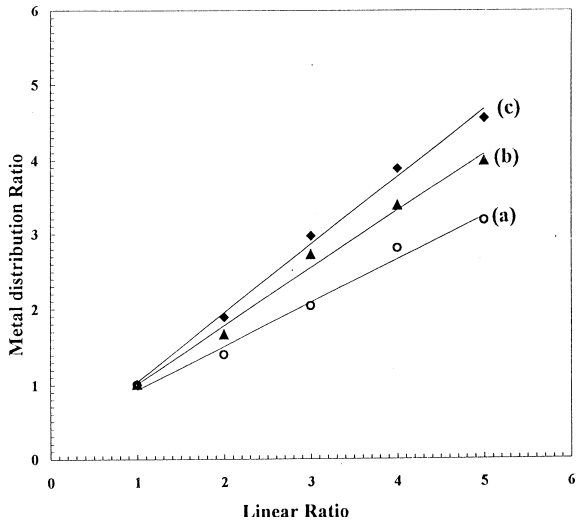

Fig. 9. Metal distribution ratio (m) against linear ratio (l), for Co3.d bath at different current density; curves: (a) 0.66, (b) 1.33 and (c) 2.0 A dm^{-2}.

on the throwing power was studied. P_{throw} increases from −9.2% (I_{throw} = 0.85) to 5.9% with increasing boric acid content from 10 to 30 g dm^{-3}. Under the chosen plating conditions of t = 15 min, i = 2.0 A dm^{-2} and at 25 °C, the P_{throw} has a low value of 5.9%. The influence of pH on the throwing power was also investigated. Increasing pH from 2.0 to pH 5.0, leads to a remarkable increase in P_{throw} from −50.1% (I_{throw} = 0.32) to 25% (I_{throw} = 1.59). This improvement may be attributed to the increase in cathodic polarization with increasing pH.

However, increasing the current density from 0.66 to 2.0 A dm^{-2}, decreases the throwing power of the bath from 29.6% to 5.9%, as a result of increased cathodic polarization. Similarly, the throwing index decreases from 1.74 to 1.10 as current density changes from 0.66 to 2.0 A dm^{-2} (Figure 9).

Raising the bath temperature from 25 to 50 °C lowers the throwing power of the bath from 5.9 to −6.9% (I_{throw} = 0.72). This is due to the decrease of cathodic polarization with increasing temperature. It is obvious that the values of the throwing power and throwing index change in a parallel manner to those calculated for P_{throw}.

3.6. *Microhardness*

The Vickers microhardness H_v (kg f mm^{-2}) for some as-deposited cobalt coatings from gluconate baths on steel were measured under different operating conditions. The data reveal that the microhardness of cobalt deposited from gluconate baths is higher than the microhardness of cobalt deposited, under similar conditions, from sulfate, chloride, bromide and acetate baths [30]. Increasing the concentration of gluconate content in the bath from 50 (Co2.f bath) to 100 g dm^{-3} (Co.2h bath) results in a decrease in the microhardness of the deposit from 416 to 341 kg f mm^{-2} (×10 MPa). The same effect was produced by introducing boric acid in the bath. The microhardness of the as-deposited cobalt, from the optimum Co3.d bath, is significantly increased with increase in current density. Increasing the current density promotes grain growth and impedes grain nucleus generation (Table 2).

Changing the pH of the bath from pH 2.0 to pH 5.0 has no significant effect on the microhardness of the as-deposited cobalt as shown in Table 2. However, the microhardness increases with increase in bath temperature.

3.7. *Crystal structure and surface morphology of the deposits*

Figure 10 shows X-ray diffraction patterns of the as-deposited cobalt obtained from the optimum (Co.3d) bath onto steel under different operating conditions. A (110)-oriented h.c.p. (α-Co) and (111)-oriented f.c.c. (β-Co) phases were observed in all films studied. It is evident that Co film deposited from the optimum bath at 2 A dm^{-2} and at pH 3.5 is composed of h.c.p. and f.c.c. phases with h.c.p. as a major phase. However, the Co deposited at higher current density (Figure 10(b)) is composed of h.c.p. and f.c.c. phases but with f.c.c. as a major phase. On the other hand, a mixture of f.c.c. and h.c.p. were produced at high pH (pH 5.0) (Figure 10(c)).

The surface morphology of the as-deposited cobalt onto steel was examined by scanning electron microscopy. Figure 11 shows the morphological details of some cobalt deposits obtained from the optimum bath under different operating variables. Compact and micro-cracked deposits were obtained from the optimum conditions. The deposits composed of fine (spherical) grains covering the entire cathode surface (Figure 11(a)). The size of the spherical grains increases with increasing the applied current density from 2.0 (Figure 11(a)) to 3.0 A dm^{-2} (Figure 11(b)). It seems that at low current densities, the nucleation rate exceeds the growth rate and the deposits were more compact with a finer grain size while at the high current densities the growth rate

Table 2. Microhardness of cobalt deposited (thickness > 10 μm) from the optimum (Co3.d) bath under different operating conditions

i/A dm^{-2} (t = 60 min, pH 3.5, 25 °C)	H_v/kg f mm^{-2} (×10 MPa)	pH (i = 2 A dm^{-2}, t = 60 min, 25 °C)	H_v/kg f mm^{-2} (×10 MPa)	Temp/°C (i = 2 A dm^{-2}, t = 60 min, pH 3.5)	H_v/kg f mm^{-2} (×10 MPa)
1.0	257	2.0	412	25	416
2.0	416	3.0	416	50	549
3.0	593	5.0	412	–	–

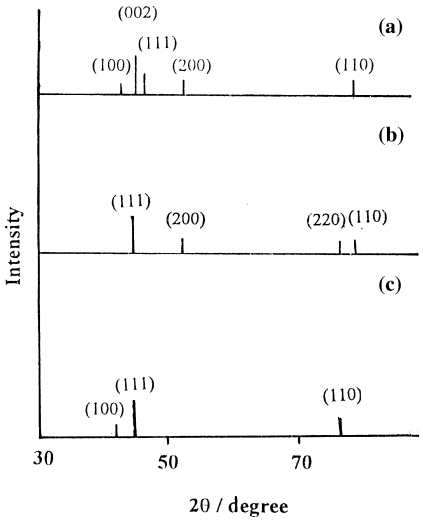

Fig. 10. X-ray diffraction patterns for the as-deposited cobalt from Co3.d bath at different operating conditions: (a) $i = 2$ A dm^{-2}, $t = 15$ min, pH 3.5 at 25 °C; (b) $i = 3$ A dm^{-2}, $t = 15$ min, pH 3.5 at 25 °C; and (c) $i = 2$ A dm^{-2}, $t = 15$ min, pH 5.0 at 25 °C.

exceeds that nucleation which results in coarse grain deposits. Decreasing the bath pH from 3.5 to 2.0 enhances the growth over the nucleation and coarse grain deposits were obtained as shown in Figure 11(c). Electrodeposition of cobalt from this bath is associated with the codeposition of hydrogen. Therefore, it can be concluded that the adsorbed hydrogen may inhibit the nucleation rate, consequently enhancing the growth rate.

On the other hand, there is a transition from spherical grain structure to dihedral fine grains of elongated shape with increasing temperature, as shown in Figure 11(d). The presence of microcracks in the deposit indicates that the deposits are highly stressed. The stress could be due to adsorption of hydrogen during cobalt deposition [25]. The density of the microcracks increases with increasing applied current density and with decreasing bath pH, but decreases with increasing bath temperature.

4. Conclusion

Electrodeposition of highly adherent and smooth deposits on a steel substrate from gluconate electrolytes was successfully achieved by using the optimum bath composition: cobalt sulfate 100, sodium gluconate 50 and boric acid 30 g dm^{-3} at pH 3.5, $i = 2$ A dm^{-2}, $t = 15$ min at 25 °C. The cathodic current efficiency is high (~95%); however, it depends on the operating conditions. The cobalt deposit obtained from this bath consists of a mixture of α- and β-cobalt. The surface morphology of the as-deposited cobalt was investigated. The cobalt deposit under the optimum conditions is composed of compact, microcracked, fine grains covering the whole substrate surface. The microhardness of the as-deposited cobalt from the present bath is generally high. The throwing power of the present bath is low ($P_{\text{throw}} \approx 5.9\%$). The data show that the electrodeposition of cobalt on glassy carbon from gluconate electro-

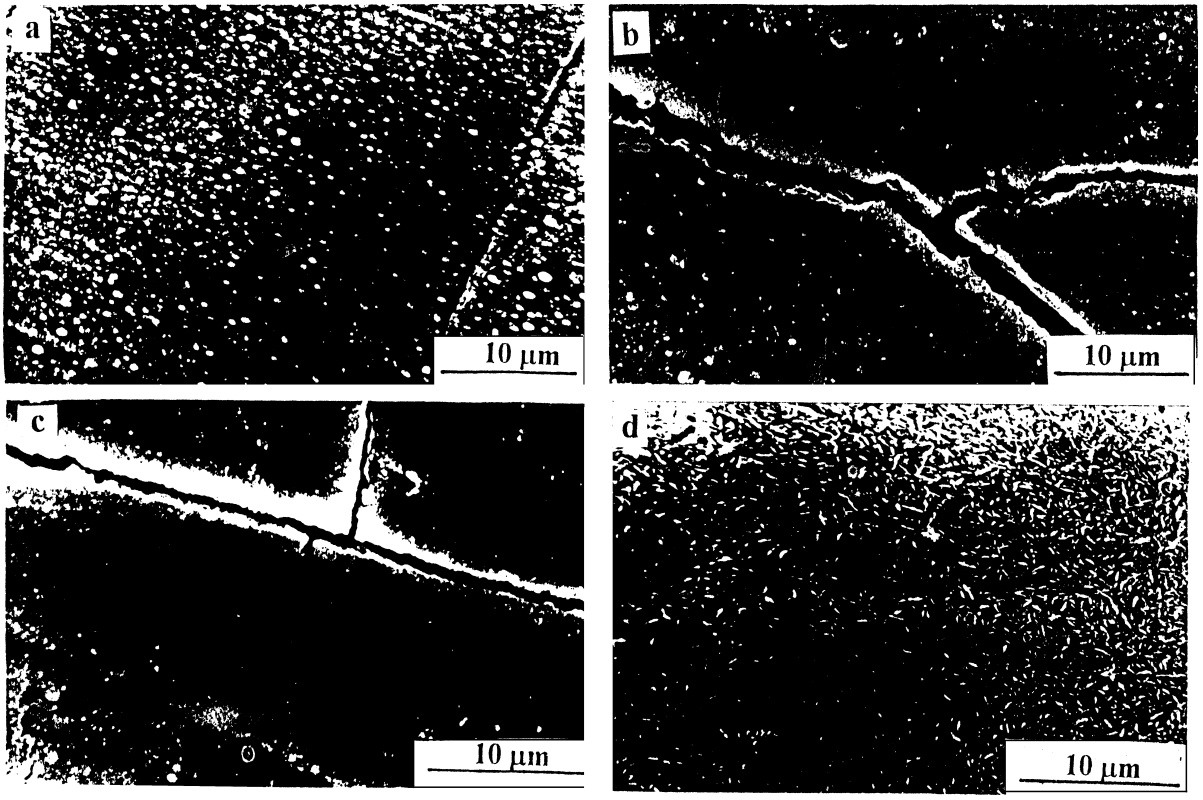

Fig. 11. Photomicrograph of cobalt deposited from Co3.d bath at: (a) $i = 2$ A dm^{-2}, $t = 15$ min, pH 3.5 at 25 °C; (b) $i = 3$ A dm^{-2}, $t = 15$ min, pH 3.5 at 25 °C; (c) $i = 2$ A dm^{-2}, $t = 15$ min, pH 2.0 at 25 °C; and (d) $i = 2$ A dm^{-2}, $t = 15$ min, pH 3.5 at 45 °C.

lyte occurs via a nucleation process under charge transfer control as indicated by the cyclic voltammetry and potentiostatic current–time techniques.

References

1. J.L. Su, M.M. Chen, J. Lo and R.E. Lee, *J. Appl. Phys.* **63** (1988) 4022.
2. H.F. Quinn and I.M. Croll, 'Advances in X-ray Analysis', Vol. 4 (Plenum Press, New York, 1980), p. 151.
3. P.N. Bartlett, P.N. Birkin, M.A. Ghanem, P. de Groot and M. Sawicki, *J. Electrochem. Soc.* **148** (2001) C119.
4. L. Peter, A. Cziraki, L. Pogany, Z. Kupay, I. Bakonyi, M. Uhlemann, M. Herrich, B. Arnold, T. Bauer and K. Wetzig, *J. Electrochem. Soc.* **148** (2001) C168.
5. I. Tabakovic, S. Riemer, V. Inture, P. Jallen and A. Thayer, *J. Electrochem. Soc.* **147** (2000) 219.
6. J.P. Celis, P. Cavallotti, J. Machado Da Silva and A. Zielonka, *Trans. Inst. Met. Finish.* **76**(5) (1998) 163.
7. J.K. Dennis, K.J. Lodge and F.A. Still, *Trans. IMF* **55** (1977) 17.
8. J.K. Dennis and D. Jones, *Surf. Technol.* **12** (1981) 57.
9. I.M. Croll and B.M. May, *in* L.T. Romanikiw and D.R. Turner (Eds), 'Electrodeposition Technology, Theory and Practice' (The Electrochem. Society Proceeding Seriers, Pennington, NJ, 1987), PV87-17, p. 295.
10. C.Q. Cui, S.P. Jiang and A.C.C. Tseung, *Electrochem. Soc.* **137** (1990) 3418.
11. A.M. Abd El Halim, M.H. Fawzy and M.A.M. Ibrahim, *Trans. Inst. Met. Finish.* **71** (2) (1993) 48.
12. S.S. Abd El Rehim, S.M. Abd El Wahaab, M.A.M. Ibrahim and M.A. Dankeria, *J. Chem. Technol. Biotechnol.* **73** (1998) 369.
13. L. Brossared, *Mater. Chem. Phys.* **27** (1991) 235.
14. C.Q. Cu, S.P. Jiang and A.C.C. Tseung, *J. Electrochem. Soc.* **138** (1991) 1001.
15. A.B. Soto, E.M. Arce, M. Palomar-Pardave and I. Gonzalez, *Electrochim. Acta* **41** (1996) 2647.
16. M. Palomar-Pardave, I. Gonzalez, A.B. Soto and E.M. Arce, *J. Electroanal. Chem.* **443** (1998) 125.
17. A. Suzaki and T. Watanabe, *J. Japan Inst. Metals* **64** (2000) 869.
18. S. Field, *Met. Ind. (London)* **44** (1934) 614.
19. R.V. Jelinek and H.F. David, *J. Electrochem. Soc.* **104** (1957) 279.
20. M.A.M. Ibrahim, *J. Chem. Technol. Biotechnol.* **75** (2000) 745.
21. C. Karwas and T. Hepel, *J. Electrochem. Soc.* **136** (1989) 1672.
22. L.G. Joyce and W.F. Pickering, *Aust. J. Chem.* **18** (1965) 783.
23. T.M. Maskin, B.Z. Znbova and D.S. Veselinovic, *J. Serb. Chem. Soc.* **56** (1991) 337.
24. S.S. Abd El Rehim, S.M. Abd El Wahaab, S.M. Rashwan and Z.M. Anwar, *J. Chem. Technol. Biotechnol.* **75** (2000) 237.
25. C. Karwas and T. Hepel, *J. Electrochem. Soc.* **135** (1988) 839.
26. J. Horkan, *J. Electrochem. Soc.* **126** (1979) 1861.
27. B. Scharifker and G. Hills, *Electrochim. Acta* **28** (1983) 879.
28. M. Gonsalves and D. Pletcher, *J. Electroanal. Chem.* **285** (1990) 185.
29. R. Greef, R. Peak, L.M. Peter, D. Pletcher and J. Robinson, 'Instrumental Methods in Electrochemistry' (Ellis Horwood, Chichester, UK, 1985), Chapter 9.
30. A.M. Abd El Halim, M.H. Fawzy and M.A.M. Ibrahim, *J. Electrochem. Soc. Jpn (Denki Kagaku)* **5** (1993) 1270.
31. E.A. Abd El Maguid, S.S. Abd El Rehim and E.M. Mostafa, *Trans. IMF* 77 (1999) 188.